View metadata, citation and similar papers at core.ac.uk

brought to you by CORE

provided by NASA Technical Reports Server

NACA RM L51E24a

NACA

RESEARCH MEMORANDUM

BUFFETING-LOAD MEASUREMENTS ON A JET-POWERED BOMBER AIRPLANE WITH REFLEXED FLAPS

By John A. See and William S. Aiken, Jr.

Langley Aeronautical Laboratory
Langley Field, Va.

NATIONAL ADVISORY COMMITTEE
FOR AERONAUTICS

WASHINGTON

August 29, 1951

NATIONAL ADVISORY COMMITTEE FOR AERONAUTICS

RESEARCH MEMORANDUM

BUFFETING-LOAD MEASUREMENTS ON A JET-POWERED BOMBER AIRPLANE WITH REFLEXED FLAPS

By John A. See and William S. Aiken, Jr.

SUMMARY

Buffet boundaries, buffeting-load increments for the stabilizers and elevators, and buffeting bending-moment increments for the stabilizers and wings as measured in gradual maneuvers for a jet-powered bomber airplane equipped with reflexed flaps and ailerons and tail-tip-incidence changes are presented and compared with similar results for the original airplane configuration. The buffeting-load increments were determined from strain-gage measurements at the roots or hinge supports of the various surfaces considered. The Mach numbers of the tests ranged from 0.35 to 0.81 at pressure altitudes close to 30,000 feet. The predominant buffeting frequencies were close to the natural frequencies of the structural components. The magnitudes and trends of buffeting-load coefficients with Mach number for the reflexed-flap configuration were similar to those for the original configuration. At low Mach numbers the magnitude of the maximum stabilizer buffet-load coefficients for the reflexed-flap configuration appeared to increase with length of time in buffeting.

INTRODUCTION

In order to obtain information concerning the aerodynamic loads and load distributions on a high-speed, relatively flexible jet-bomber airplane, a flight investigation has been conducted on a North American B-45A by the National Advisory Committee for Aeronautics. The results from the program are to be used to check the validity of available computational methods and small-scale wind-tunnel measurements of items such as the aerodynamic center and the zero-lift pitching-moment coefficient of the wing-fuselage combination. References 1 to 7 present results in time-history form of some of these tests.

Concurrently with these tests, airplane buffeting was experienced at several combinations of Mach number, normal-force coefficient, and altitude. Reference 8 contains some of the buffeting results obtained during the portion of the program applicable to the original B-45A configuration. In accordance with Air Force technical-order changes, several modifications have been made to the airplane since the tests reported in reference 8. This paper presents comparisons of the buffeting-boundary, buffeting loads, and moment coefficients for the original configuration and the modified configuration with reflexed flaps and ailerons and tail-tip-incidence changes.

SYMBOLS

C_N	normal-force coefficient $\left(\frac{\text{Load}}{qS}\right)$
C_{BM}	bending-moment coefficient $\left(\frac{BM}{qS\frac{b}{2}}\right)$
BM	bending moment, inch-pounds
q	dynamic pressure, pounds per square foot $\left(0.7pM^2\right)$
p	free-stream static pressure, pounds per square foot
n	airplane load factor, g units
M	Mach number
W	airplane weight, pounds
S	area of component being considered, square feet
b/2	semispan of component being considered, inches
a	slope of lift curve, taken as 4.63 per radian
ρ_o	mass density of air at sea level, slugs per cubic foot
V_e	equivalent airspeed, feet per second
U_e	effective gust velocity, feet per second

K gust alleviation factor, taken as 1.2

Δ when used with coefficients denotes incremental values

Subscripts:

A airplane

T horizontal tail

E elevator

W wing

B buffet

cg center of gravity

APPARATUS AND TESTS

Airplane

The airplane used for this investigation is a B-45A and is shown in a three-view line drawing in figure 1. Included in the figure are the approximate locations of the bending-moment and shear strain-gage bridges. Some of the pertinent characteristics of the test airplane are given in table I. In accordance with Air Force technical orders the following modifications have been made to the airplane since the tests reported in reference 8. The wing flaps were reflexed and a bent-down trailing-edge strip was added as shown schematically in figure 2 in comparison with the original airfoil (NACA 66,2-215) flap contour. In addition to the reflexed flap, the ailerons were uprigged $3^{\circ}48'$ and end plates added to the flap-fuselage and flap-nacelle junctures. The tip of the horizontal tail outboard of the elevator was modified by bending down the trailing edge rearward of the rear spar 2°.

Instrumentation

Standard NACA photographic recording instruments were used to measure airspeed and altitude, rolling, pitching and yawing velocities, sideslip angle, accelerations, control forces, and control positions. Normal, transverse, and longitudinal accelerations were measured at the airplane center of gravity and at fuselage station 714 (approx. the one-quarter mean chord of the horizontal tail).

An airspeed boom was mounted at the left wing tip with the airspeed head approximately 1 local chord ahead of the leading edge of the wing. The results of a flight calibration of the airspeed system for position error and an analysis of available data for a similar installation indicate that the measured Mach number differs from the true Mach number by less than ±0.01 throughout the test range.

Electrical wire-resistance strain gages located on the main spars of the wing and tail surfaces were used for measuring the shear and bending moment. Each hinge of the elevator was instrumented with strain gages to measure the load. The strain-gage outputs were recorded on two 18-channel oscillographs with individual galvanometer responses flat to 60 cycles per second. A 0.1-second timer was used to synchronize all of the records.

In order to establish the relationship of the strain-gage-bridge output, as a function of shear or bending moment, calibration loads were applied to the airplane structure in the Langley aircraft loads calibration laboratory. In general the equations which were determined from the calibrations included several terms. For example, the net shear on the left side of the horizontal stabilizer was given by an equation of the form

$$\text{Net shear (left stabilizer)} = A\delta_{S_L} + B\delta_{BM_L} + C\delta_{BM_R}$$

Where A, B, and C are calibration coefficients and the δ symbols are the strain-gage responses of the left shear, left bending-moment, and right bending-moment bridges, respectively. For shear, the term $A\delta_{S_L}$ is the primary term and is the only one used to evaluate the buffeting loads inasmuch as preliminary checks showed that no significant loss of accuracy in the evaluation of the buffeting-load increments resulted from the omission of the secondary terms.

The bending moment on the horizontal stabilizers and the wing root bending moments and shears were determined in a similar manner.

During the tests on the original airplane configuration reported in reference 8, the elevator loads were measured by combining the output from the three outer hinge-bracket strain-gage bridges and the three inner hinge-bracket strain-gage bridges and then determining the elevator load from a calibration equation of the form

$$\text{Net load per side (elevator)} = A\delta_{\text{outboard}} + B\delta_{\text{inboard}} \qquad (1)$$

where A and B are calibration coefficients and the δ's are the electrically combined strain-gage-bridge responses.

In order to check the adequacy of the method of equation (1) for measuring the elevator buffeting load and also to determine the buffeting-load increments on the individual hinge brackets, some data were obtained with the reflexed-flap configuration where the load on the right elevator was determined from an electrical combination of all six hinge-bracket strain-gage bridges as

$$\text{Net load (right elevator)} = C\delta_{\text{all combined}} \tag{2}$$

The load on the left elevator was determined from individual recording of each hinge-bracket strain-gage response so that the total load on left elevator had to be evaluated from an equation of the form

$$\text{Net Load (Left Elevator)} = D\delta_1 + E\delta_2 + F\delta_3 + G\delta_4 + H\delta_5 + I\delta_6 \tag{3}$$

In equation (3) D, E, F, G, H, and I are calibration coefficients and $\delta_1, \ldots \delta_6$ are the strain-gage responses for each of the six hinge brackets. When the left elevator load was determined from electrical combination of all six bridges (equation (2)), the right elevator individual hinge-bracket loads were recorded simultaneously and the total load evaluated by means of equation (3).

Tests

All tests were made with the airplane in the clean condition. The test data fall into two classes, intentional buffeting and inadvertent buffeting. The data obtained in intentional-buffeting maneuvers were for several flights in which the pilot was specifically instructed to obtain values of airplane normal-force coefficient beyond the buffeting boundary and to allow the airplane to shake for periods of about 5 seconds. Since at the highest Mach numbers buffeting was encountered in level flight the pilot pushed down in an attempt to establish the buffet boundary. Inadvertent-buffeting data were obtained from wind-up turns where the pilot started the recovery immediately at the onset of buffeting. With the exception of two runs at approximately 20,000 feet all the buffeting data were obtained at 30,000 feet pressure altitude.

RESULTS AND DISCUSSION

Buffet Boundary

The criterion used to establish the gradual-turn buffet boundary was an incremental change in tail load of ±200 pounds per side. It was found from the flight tests on the original airplane configuration reported in reference 8 that when the pilot intentionally approached buffeting the value chosen as the criterion coincided with the pilot's opinion of onset of buffeting.

The gradual-turn buffet-boundary data for the test airplane with reflexed flaps, ailerons, and tail-incidence changes are shown in figure 3 in terms of airplane normal-force coefficient C_{N_A} and Mach number M. In several of the higher Mach number runs buffeting was continuous, in which case the minimum C_{N_A} obtained with buffeting still present is shown by inverted triangles. In order to help in defining the curve, several points are shown where no buffeting was obtained. The maximum values of C_{N_A} reached in these cases are shown as triangles. In one instance, rough air was encountered during the maneuver where an attempt was being made to reach buffeting. The data obtained during the rough-air run are shown on the appropriate figures and are discussed in detail in the section entitled "Rough Air." In figure 3 the onset of airplane oscillation due to rough air is shown as a square at the Mach number of approximately 0.73 and a C_{N_A} of 0.62.

During the process of obtaining loads information at 20,000 feet pressure altitude, inadvertent buffeting occurred during two runs. While it is impossible from the meager buffeting information at this altitude to draw any definite conclusions, the data seem to indicate that a marked reduction occurs in the buffet boundary at 20,000 feet at the high Mach numbers.

The faired buffet boundary shown in figure 3 is similar to others obtained for airplanes having unswept laminar flow or low-drag wings. A typical depression occurs around Mach number 0.53 with a peak around 0.69, followed by a sharp drop to zero airplane normal-force coefficient around 0.80 Mach number. For the gross weight and altitude at which the test airplane was flown it was impossible to obtain buffeting between Mach numbers of approximately 0.67 and 0.74 without exceeding the test-program limitations of $n = 3.0$.

The buffet boundary for the reflexed-flap airplane from figure 3 is compared in figure 4 with the buffet boundary for the original

configuration from reference 8. Both curves are for the clean condition at approximately 30,000 feet pressure altitude. At Mach numbers below M = 0.72 the reflexed-flap-configuration buffet boundary is apparently reduced while at values of Mach number above M = 0.72 airplane buffeting is delayed until a higher value of airplane normal-force coefficient is reached.

Buffeting-Load Increments

While the basic strain-gage equations for evaluating the net structural horizontal-tail load, as mentioned previously, consists of three terms, only the primary term was used for evaluating the oscillatory buffeting-load increments. In order to compare the use of the one-term and three-term equations for shear, figure 5 presents portions of representative time histories of the net structural loads on the horizontal stabilizers during a gradual turn at a Mach number of 0.44 and a pressure altitude close to 30,000 feet.

Two curves are shown, where the circles represent the load on the stabilizer using all the terms in the basic equation such as

$$\text{Net load left side (horizontal stabilizer)} = A\delta_{S_L} + B\delta_{BM_L} + C\delta_{BM_R}$$

The squares represent the load measured using only the primary term in the expression where

$$\text{Net load left side (horizontal stabilizer)} = A\delta_{S_L}$$

A maximum net structural buffeting-load increment of 3,330 pounds is shown in figure 5 for the left horizontal stabilizer using all of the coefficients in the equation while a maximum net structural buffeting-load increment of 3,220 pounds is shown for the same surface using only one coefficient. Similar results are shown for the right stabilizer. For this particular case there seems to be no significant difference between the maximum buffet-load increments evaluated by the two methods.

Horizontal-stabilizer shear.- The incremental buffeting loads on the horizontal stabilizer were determined for each buffeting run using only the maximum double amplitude on both the left and right horizontal stabilizers. These buffeting increments on the stabilizers were converted to coefficient form by use of the expression

$$\Delta C_{N_{T_B}} = \frac{\text{Load}}{qS_T}$$

where the load in this case corresponds to the double amplitude as measured from the strain-gage records.

Data similar to those shown in figure 5 using only the primary term were used in the preparation of figure 6 where the horizontal-stabilizer buffeting-load coefficient is plotted against Mach number. In figure 6 the circles represent the values obtained for the left stabilizer and the squares represent those for the right stabilizer. In order to distinguish between intentional and inadvertent buffeting a cross superimposed on the circle or square indicates intentional buffeting. All of the points shown in figure 6 were obtained with the reflexed-flap configuration and a boundary (from reference 8) is shown for the original airplane test configuration. From figure 6 it can be seen that the magnitude of the buffeting loads obtained during intentional buffeting are larger than those during inadvertent buffeting where recovery was made rather abruptly. This result suggests that the magnitude of the buffeting load may be dependent on the time in buffeting before the pilot executes a recovery.

A comparison of the boundary line (as given in reference 8) for the original configuration with the test data for the modified configuration in figure 6 indicates that there is no appreciable change in the maximum buffeting loads measured. The data obtained at 20,000 feet fall considerably below those obtained for either inadvertent or intentional buffeting at 30,000 feet.

Stabilizer bending moment.- The stabilizer bending-moment coefficients obtained during buffeting are shown in figure 7. A distinction is again made between the left and right sides and intentional and inadvertent buffeting. The bending-moment coefficient shown for the stabilizer is defined as

$$\Delta C_{BM_{T_B}} = \frac{\text{Bending moment}}{qS_T \frac{b_T}{2}}$$

where the bending moment is the maximum double amplitude for each maneuver. Only the portion of the bending moment measured by the bending-moment bridge on either the left or right side is considered. The values of bending-moment increments obtained during intentional buffeting are generally higher than during inadvertent buffeting. There is no significant difference between the values for the left and right tail. Several of the maximum incremental bending-moment values obtained for the original configuration (fig. 8, reference 8) are shown for comparison. The figure indicates that the magnitudes of the maximum incremental bending-moment coefficients are comparable for the two configurations. The buffeting bending-moment coefficients obtained at 20,000 feet fall below those obtained at 30,000 feet.

Wing bending moment.- Left- and right-wing buffeting bending-moment coefficients as a function of Mach number are plotted in figure 8. A distinction is again made between the left and right wings and inadvertent and intentional buffeting. The wing bending-moment coefficient shown is defined as

$$\Delta C_{BM_{W_B}} = \frac{\text{Bending Moment}}{qS_W \frac{b_W}{2}}$$

where the bending moment is the maximum double-amplitude measurement for each maneuver while in buffeting. Only the part of the bending moment measured by the bending-moment bridge on either the left or right side is considered. In nearly all cases the incremental bending moment was higher for intentional buffeting than inadvertent buffeting while similarity in the magnitude exists between the left and right wings. For a comparison of the two configurations several points obtained for the original airplane configuration (from fig. 9, reference 8) are shown.

The wing buffeting bending-moment coefficients obtained at 20,000 feet are considerably lower than those obtained at 30,000 feet.

Wing structural shear buffet increments are not shown because in all cases, for both inadvertent and intentional buffeting, the structural load was less than ±1,000 pounds. The estimated reading accuracies for the wing shear are ±400 pounds; therefore, the results for the wing-shear buffeting increment have not been included.

Elevator load.- As described under the section "Instrumentation" the elevator buffeting-load increments have been measured using three different recording systems with the structural loads obtained from equations of the form

$$\text{Net load per side (elevator)} = A\delta_{outer} + B\delta_{inner} \quad (1)$$

$$\text{Net load (right elevator)} = C\delta_{\text{all combined}} \quad (2)$$

$$\text{Net load (left elevator)} = D\delta_1 + E\delta_2 + F\delta_3 + G\delta_4 + H\delta_5 + I\delta_6 \quad (3)$$

In previously reported results (reference 8), equation (1) was used for evaluating the elevator buffeting-load increments, while for the reflexed-flap configuration the three recording systems were used at various times during the test program.

The results of measuring the elevator buffeting-load increments by the use of equations (2) and (3) are shown in table II. This table

presents the maximum left elevator hinge-bracket buffeting-load increments for hinges 1 to 6 obtained during buffeting at Mach numbers from 0.38 to 0.81, the summation of these loads (equation (3)), and the maximum buffet-load increments for the right elevator (from equation (2)). All data given in table II are for a pressure altitude of 30,000 feet and the loads in pounds are double-amplitude structural buffeting increments.

Although the time of occurrence in the maneuver of the various peak loads listed for each Mach number was not the same, the agreement between the results using equation (2) or equation (3) was reasonably good. The summation of loads (equation (3)), on the left elevator was higher on the average than the recorded total load for the right elevator; however, due to the method of obtaining the total structural load on the left elevator, no significance should be attached to this result.

The left- and right-elevator buffeting-load coefficients for both inadvertent- and intentional-buffeting maneuvers are shown in figure 9 as a function of Mach number. The elevator load coefficient is expressed as

$$\Delta C_{N_{E_B}} = \frac{\text{Load}}{qS_E}$$

where the load is the double amplitude for one elevator during buffeting and the elevator area includes both elevators.

Loads measured using equations (1), (2), and (3) are presented in the figure, where the squares are for equation (2) having all of the gages on the right combined, and circles are for equation (3) for summation of individual hinge loads on the left. Triangles and diamonds represent loads measured using equation (1) for the left and right sides, respectively. The points shown as open symbols were obtained during inadvertent buffeting while the crossed symbols are for intentional buffeting. Again the loads measured on the left or right elevator are not significantly different, but loads obtained during intentional buffeting are generally higher than those for the inadverent cases. Elevator buffeting-load increments obtained at 20,000 feet are lower than those obtained at 30,000 feet.

The faired boundary line obtained for the original configuration (fig. 10, reference 8) is shown in figure 9. Although several points obtained with the reflexed-flap configuration are above the previous boundary, these points would be expected to be higher due to the method of measurement of the loads on the left elevator.

Since the elevator buffet-load increments are being measured by means of strain-gage bridges on the hinge-bracket supports, it is not possible to separate for buffeting conditions the part of the load on these brackets which is due to bending of the stabilizer and the part due to the actual load on the elevator. Even if most of the load on the hinges were due to elevator load, a part of it would be due to the inertia of the mass balances which would effect only the torque tube and hinge-bracket stresses.

Extrapolation of Buffeting Loads

No extrapolation of the load coefficients to loads at various altitudes has been made in the present paper since some doubt exists as to the validity of the assumption that the loads for a given Mach number are directly proportional to the dynamic pressure. This doubt has arisen since the issuance of reference 8. Unpublished results of buffeting-load measurements on the F-51D airplane have indicated that, at Mach numbers below $M = 0.65$, the damping of the vibrating structure may be increasing rapidly enough with increasing air density so as partially to offset the increasing magnitude of the forcing function of buffeting.

Buffeting and Structural Frequencies

A marked similarity exists between the structural natural frequencies and the frequencies measured from the strain-gage records during buffeting. Table III lists some pertinent airplane structural frequencies obtained primarily from vibration tests conducted on a North American XB-45 airplane at Wright Patterson Air Force Base (reference 9). Since the tail span is longer by several feet than the one tested by the Air Force, the tail bending frequency listed in the table was obtained in ground tests at the Langley Aeronautical Laboratory.

The lower part of table III lists the most pronounced frequencies that were present with the strain-gage record from which they were obtained. As far as can be determined these frequencies are the same as those estimated for the original configuration. The wing bending gages showed a frequency very close to 4 cycles per second with occasional low-amplitude oscillations near 10 and 14 cycles per second. The stabilizer shear and bending strain-gage records were composed mainly of oscillations at 4, 6, 10, and 36 cycles per second. The elevator shear-gage records were mainly composed of oscillations at 6 and 36 cycles per second.

During buffeting maneuvers the wings were generally oscillating in phase but the left- and right-stabilizer load oscillations were out

of phase as often as in phase. An illustration of the phase relationship for left and right horizontal stabilizers is shown in figure 5 where the loads in buffeting on the two sides are almost 180° out of phase. The loads measured on individual elevator hinge brackets were out of phase as often as in phase regardless of the recording system used. For the left elevator where individual hinge loads were measured, the maximum buffeting loads seldom, if ever, occurred simultaneously on all six hinges.

Time in Buffeting

An effect of length of time in buffeting is shown in figure 10 where the stabilizer load coefficient is given as a function of time in buffeting. Time in buffeting is considered as the time required to reach the maximum value of incremental buffeting load after the initial start of buffeting. The left and right sides of the stabilizer are distinguished by circles and squares. For the three runs illustrated the average Mach number was 0.45. For each condition the change in the airplane normal-force coefficient $\left(\Delta C_{N_A}\right)$ between start of buffeting and maximum attained buffeting load is also shown. No correlation appears to exist between $\Delta C_{N_{T_B}}$ and ΔC_{N_A}, but the figure indicates that $\Delta C_{N_{T_B}}$ increases with time in buffeting. No conclusions should be drawn from the data of figure 10 concerning relative effects of penetration beyond the buffet boundary and time in buffeting for higher Mach numbers. Tests on other airplanes have indicated that, in the Mach number range where buffeting is encountered before maximum lift is reached, some correlation exists between penetration beyond the buffet boundary and the magnitude of buffeting loads; however, in the present case penetration beyond the buffet boundary at high Mach numbers was not sufficient to permit a similar analysis.

Rough Air

Rough air was encountered during one flight at a pressure altitude of approximately 30,000 feet and a Mach number of 0.73. Using the effective-gust-velocity equation presented in reference 10 where

$$\Delta n_{cg} = \frac{\rho_o a K U_e V_e S_W}{2W}$$

the value for U_e during rough air was found to equal 8.8 feet per second. The assumption made herein is that the measured center-of-gravity acceleration represents the airplane acceleration.

The maximum horizontal-stabilizer shear and bending-moment coefficients and, wing bending-moment and elevator load coefficients obtained in the rough-air run are shown in figures 6, 7, 8, and 9, respectively. The stabilizer and elevator coefficients are of the same magnitude as those obtained during inadvertent buffeting. The wing bending-moment coefficient obtained during rough air was considerably higher than the intentional or inadvertent buffeting coefficients obtained at corresponding Mach numbers with an absolute value of ±480,000 inch-pounds, a value higher than any wing buffeting bending-moment increments.

The wing bending-moment strain-gage records had different characteristics in rough air than during buffeting; in rough air the wing vibration appeared to be purely at the first fundamental bending frequency of the wing.

SUMMARY OF RESULTS

The gradual-maneuver buffet boundary, as established by the onset of buffeting from strain-gage records, appears to be similar to that of other airplanes with low-drag airfoils. Reflexing the flaps and ailerons and changing the tail-tip incidence did not materially affect the buffet boundary for the test airplane as compared with the buffet boundary for the original configuration.

Buffeting-load increments determined by the use of only the primary shear or bending-moment strain-gage bridge showed no significant differences from those determined using all bridges normally needed to establish tail loads.

The loads measured during buffeting were generally higher for intentional buffeting conditions as compared with inadvertent buffeting.

At lower Mach numbers the magnitude of the maximum stabilizer buffeting-load coefficients appeared to increase with length of time in buffeting.

A comparison of the buffeting-load coefficients for the reflexed-flap airplane and the original configuration indicated that stabilizer buffeting load and bending-moment coefficients were essentially the same for the two configurations.

Elevator buffet-load coefficients for the two configurations showed the same trend with Mach number; however, where the loads were measured using the individual hinge-bracket-load summations some of the

reflexed-flap-configuration load coefficients were higher than the boundary established for the original configuration.

Wing bending moments and shears measured during buffeting were relatively small, and incremental shears never exceeded ±1,000 pounds.

Since some doubt exists at the present time as to the method of extrapolating buffet-load data to low altitudes, no conclusions are drawn concerning the occurrence of critical loads on the stabilizer and elevator.

The buffeting frequencies estimated from the strain-gage records indicated a definite similarity with the structural natural frequencies. The left and right elevator and stabilizer were at times in phase and at times out of phase while the left and right wings were generally inphase with one another during buffeting.

In rough air at a Mach number of 0.73 the incremental oscillatory loads on the stabilizer and elevator were in general less than those measured during buffeting at the same Mach number. For the wing the incremental bending moment in rough air was higher than any values measured during buffeting at any Mach number. In rough air the wing vibration was at the first fundamental bending frequency whereas during buffeting other frequencies were superposed on the fundamental vibration.

Langley Aeronautical Laboratory
National Advisory Committee for Aeronautics
Langley Field, Va.

REFERENCES

1. Aiken, William S., Jr., and Wiener, Bernard: Time Histories of Horizontal-Tail Loads on a Jet-Powered Bomber Airplane in Four Maneuvers. NACA RM L9H16a, 1949.

2. Cooney, T. V., and McGowan, William A.: Time Histories of Loads and Deformations on a B-45A Airplane in Two Aileron Rolls. NACA RM L9I28a, 1949.

3. Cooney, T. V., and Aiken, William S., Jr.: Time Histories of the Loads and Deformations on the Horizontal Tail of a Jet-Powered Bomber Airplane in Accelerated Maneuvers at 30,000 Feet. NACA RM L50B24a, 1950.

4. McGowan, William A., and Wiener, Bernard: Time Histories of Horizontal-Tail Loads and Deformations on a Jet-Powered Bomber Airplane during Wind-Up Turns at 15,000 Feet and 22,500 Feet. NACA RM L50C21a, 1950.

5. McGowan, William A.: Time Histories of Horizontal-Tail Loads, Elevator Loads, and Deformations on a Jet-Powered Bomber Airplane during Wind-Up Turns at Approximately 15,000 Feet and 22,500 Feet. NACA RM L50F28, 1950.

6. Wiener, Bernard, and Harris, Agnes E.: Time Histories of Horizontal-Tail Loads, Elevator Loads, and Deformations on a Jet-Powered Bomber Airplane during Abrupt Pitching Maneuvers at Approximately 20,000 Feet. NACA RM L50J05a, 1950.

7. Cooney, T. V., and McGowan, William A.: Time Histories of the Aerodynamic Loads on the Vertical and Horizontal Tail Surfaces of a Jet-Powered Bomber Airplane during Sideslip Maneuvers at Approximately 20,000 Feet. NACA RM L51A08, 1951.

8. Aiken, William S., Jr., and See, John A.: Strain-Gage Measurements of Buffeting Loads on a Jet-Powered Bomber Airplane. NACA RM L50I06, 1951.

9. Mykytow, Walter J.: Vibration Inspection and Flutter Analyses of the North American XB-45 Airplane. Ser. No. TSEAC5-4262-25-34, Air Materiel Command, Army Air Forces, May 20, 1947.

10. Donely, Philip: Summary of Information Relating to Gust Loads on Airplanes. NACA Rep. 997, 1950. (Formerly NACA TN 1976.)

TABLE I

CHARACTERISTICS OF TEST AIRPLANE

Wing:	
Span, feet	89.04
Area, square feet	1175
Mean aerodynamic chord, feet	14.02
Airfoil, root	NACA 66,2-215
Airfoil, tip	NACA 66,1-212
Taper ratio	2.42
Horizontal tail surfaces:	
Area (including fuselage), square feet	289.44
Span, feet	43.87
Elevator:	
Area (including tabs), square feet	67.71
Gross weight, pounds (range as flown)	55,000 to 63,000
Center of gravity (range as flown), percent M.A.C.	26.4 to 28.2

TABLE II

COMPARISON OF ELEVATOR AND ELEVATOR HINGE-BRACKET MAXIMUM DOUBLE AMPLITUDE BUFFET-LOAD INCREMENTS MEASURED AT 30,000 FEET

Mach number	Individual hinge-bracket loads on left elevator (hinge location - in. from center line) (lb)						Left elevator load using equation (3) (summation of individual hinge loads) (lb)	Right elevator load using equation (2) (all strain gages combined electrically) (lb)
	Hinge 1 ($20-\frac{5}{16}$ in. from center line)	Hinge 2 ($51-\frac{1}{2}$ in. from center line)	Hinge 3 (92 in. from center line)	Hinge 4 (133 in. from center line)	Hinge 5 (175 in. from center line)	Hinge 6 (216 in. from center line)		
0.377	370	510	590	800	580	240	3090	3200
.399	430	740	920	960	790	230	4070	3960
.409	250	300	530	700	560	190	2530	2340
.439	460	830	1620	1170	900	330	5310	4180
.453	370	550	840	800	670	220	3450	2760
.478	270	400	600	530	720	220	2740	1860
.491	190	180	430	510	400	170	1880	1750
.514	250	270	490	540	400	170	2120	1700
.544	210	150	450	510	350	170	1840	1170
.568	180	120	400	390	270	150	1510	850
.599	140	200	440	300	280	120	1480	1410
.607	140	170	360	400	250	130	1450	740
.637	450	970	1730	1370	830	330	5680	3690
.638	350	520	840	760	670	260	3400	1910
.664	180	300	480	590	430	150	2130	3040
.725[a]	70[a]	120[a]	170[a]	140[a]	130[a]	30[a]	660[a]	760[a]
.744	110	120	210	270	210	140	1060	950
.750	110	140	220	230	260	80	1040	1090
.762	120	180	280	310	350	110	1350	1060
.794	180	270	530	530	550	250	2310	2120
.795	270	480	700	510	710	300	2970	1850
.809	390	1030	940	850	1020	450	4680	3500

[a]Rough air.

TABLE III

FREQUENCY CHARACTERISTICS

Natural frequencies of airplane components (cps):	
Wing:	
First symmetrical bending	4.6
Unsymmetrical wing bending and inner-panel torsion	9.2
Second symmetrical bending	14.3
Fuselage:	
Torsion and side bending (primarily torsion)	4.3
Vertical bending	8.0
Horizontal stabilizer:	
Primary bending (symmetrical)	6.7
Torsion	36.7
Elevator:	
Torque tube torsion	14.2
Symmetrical rotation	8.3 to 10.0
Buffeting frequencies estimated from records for the following strain-gage bridges (cps):	
Wing bending	4, 10, 14
Stabilizer shear	4, 6, 10, 36
Stabilizer bending	4, 5, 6, 10, 36
Elevator shear	6, 36

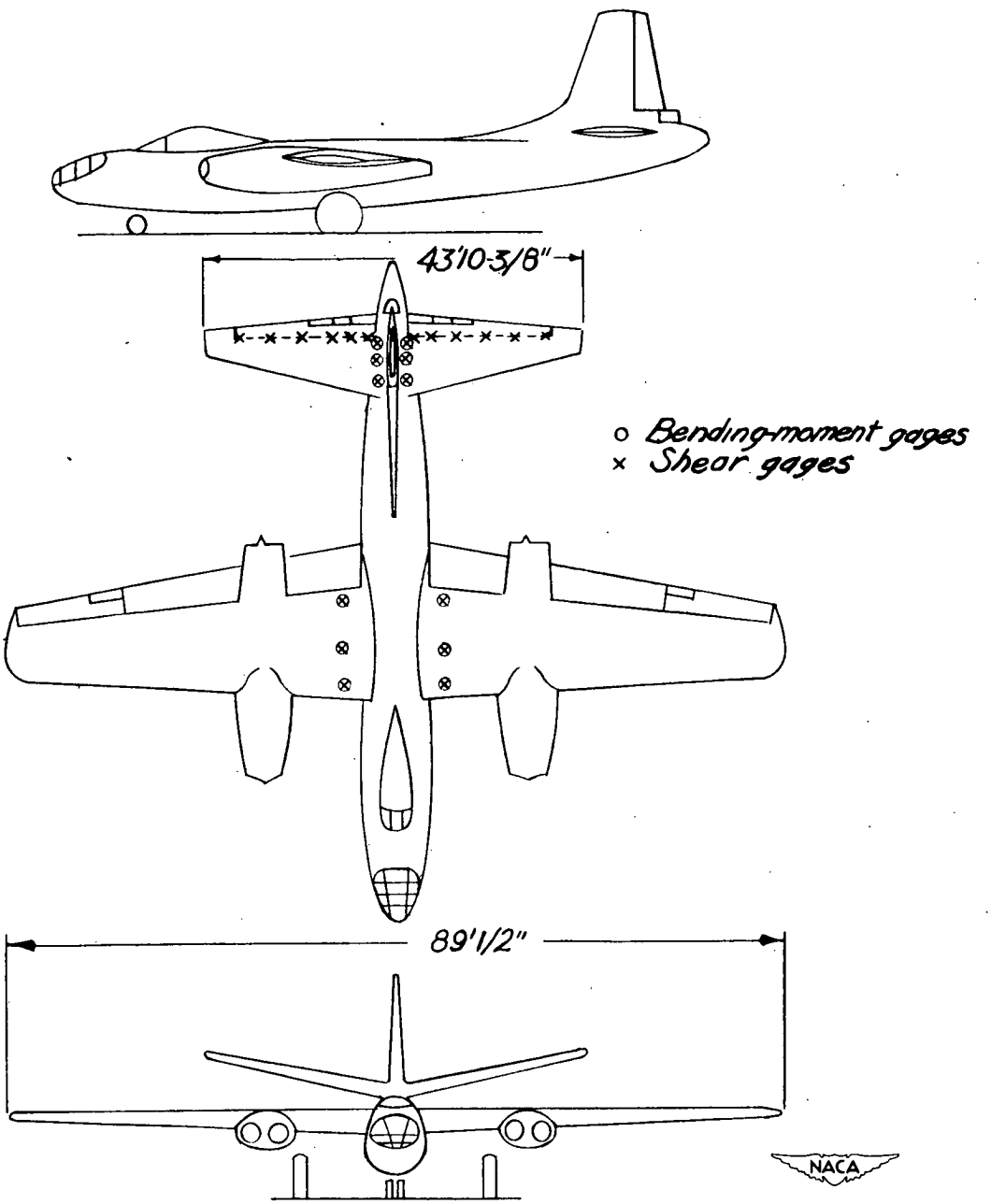

Figure 1.- Three-view drawing of test airplane showing approximate locations of strain-gage bridges.

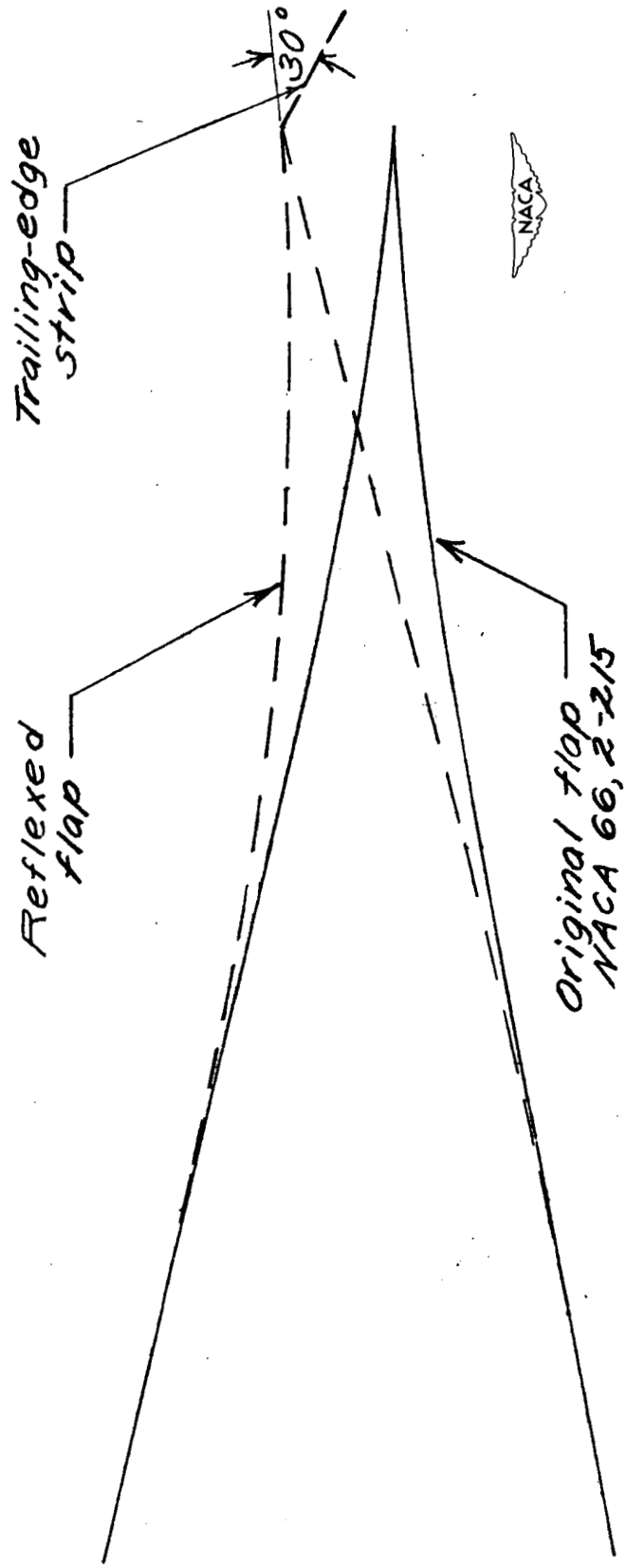

Figure 2.- Original- and reflexed-flap profile.

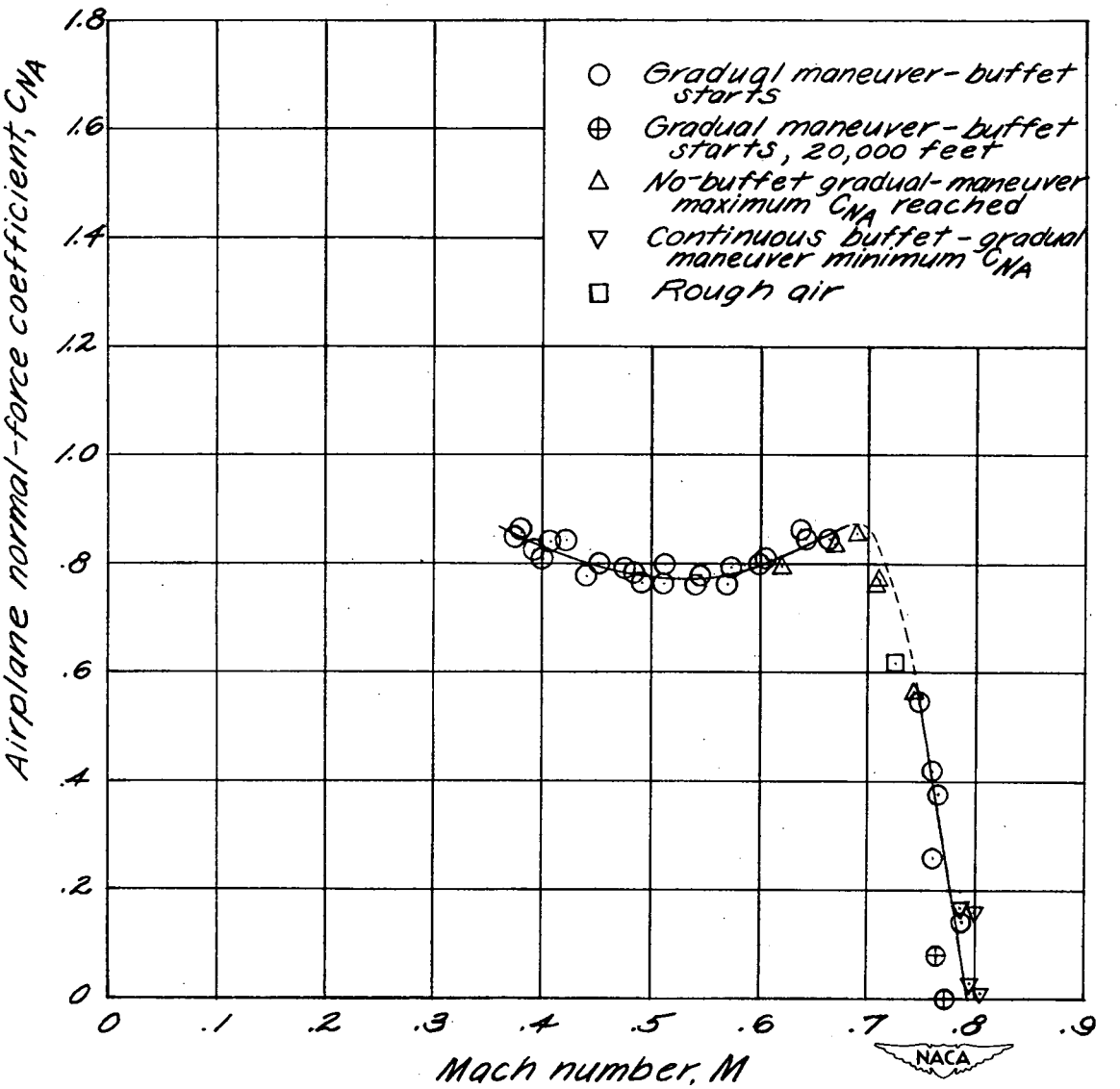

Figure 3.- Buffet boundary for test airplane with reflexed flaps.

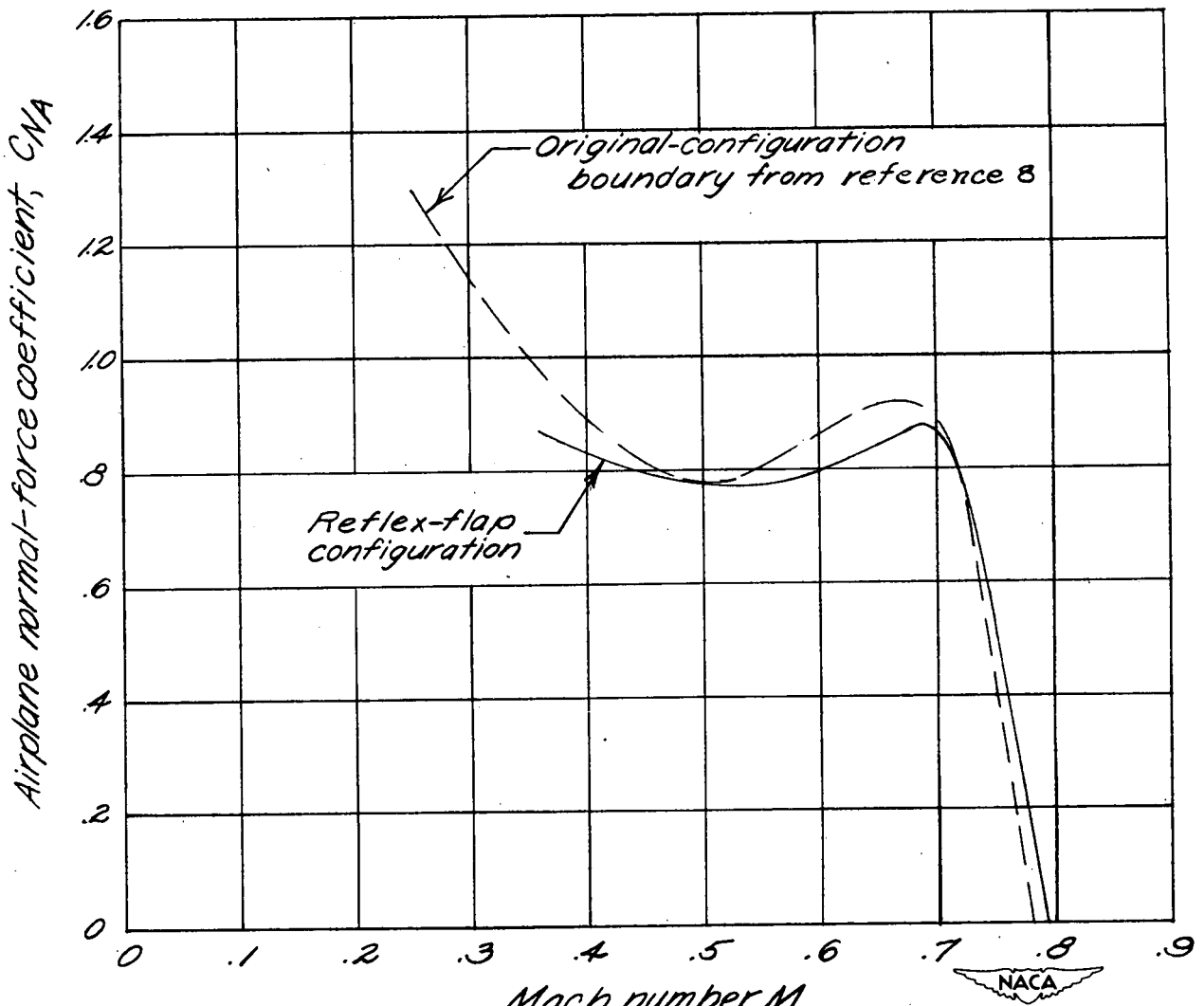

Figure 4.- Comparison of gradual-turn buffet boundaries for test airplane.

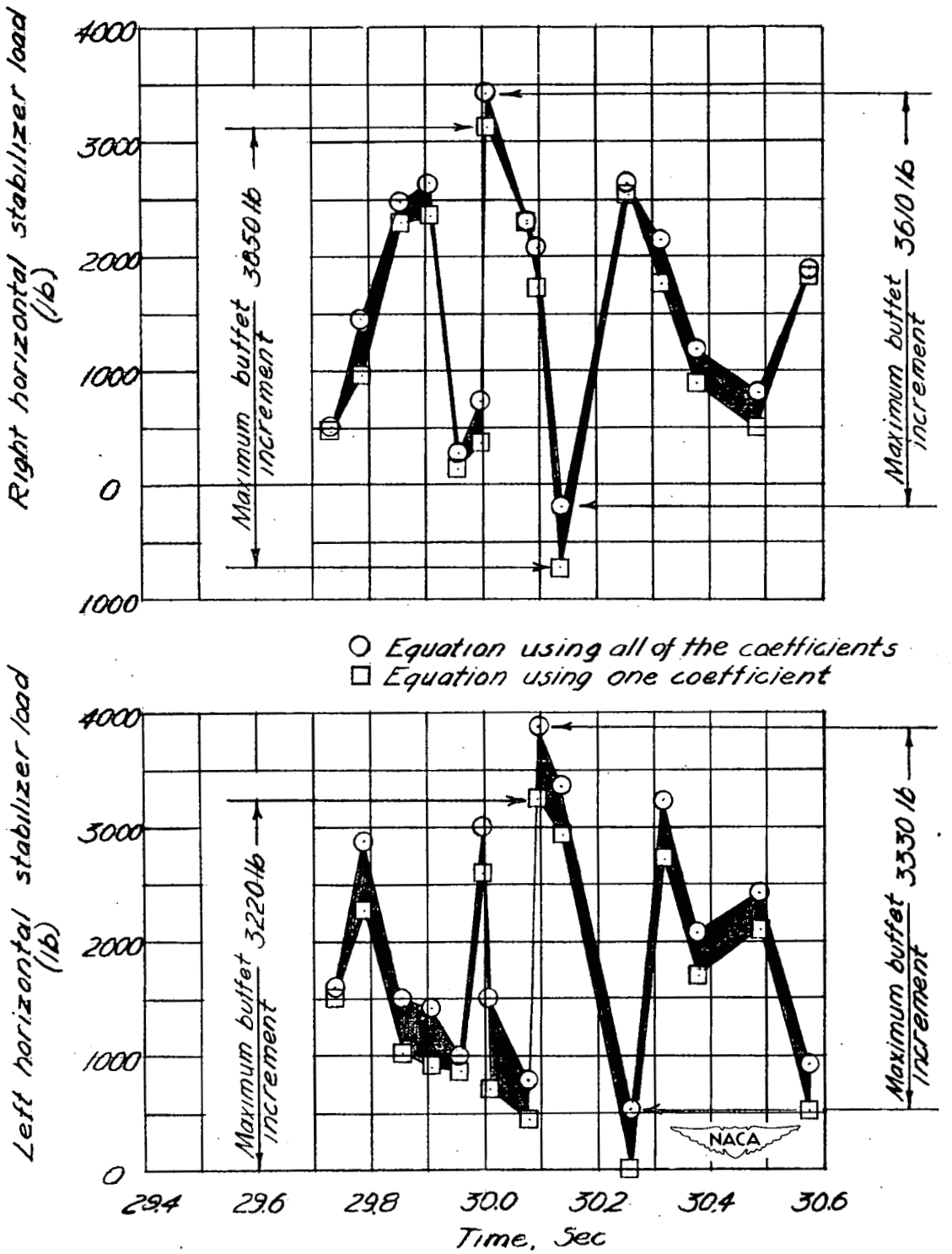

Figure 5.- Comparison of time histories of stabilizer buffeting loads obtained by two methods of evaluating strain-gage data. M = 0.44; pressure altitude, 30,000 feet.

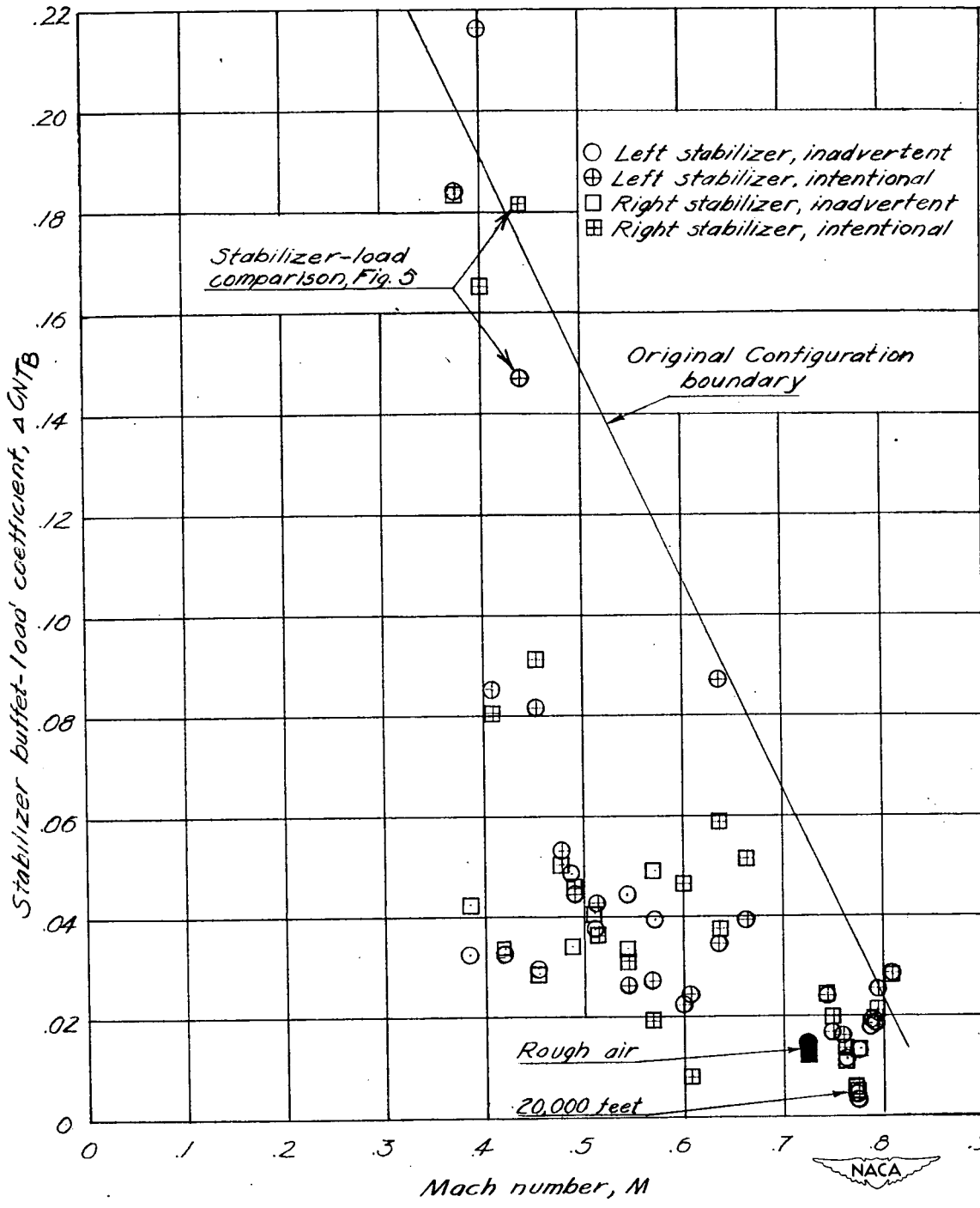

Figure 6.- Stabilizer buffeting-load coefficients.

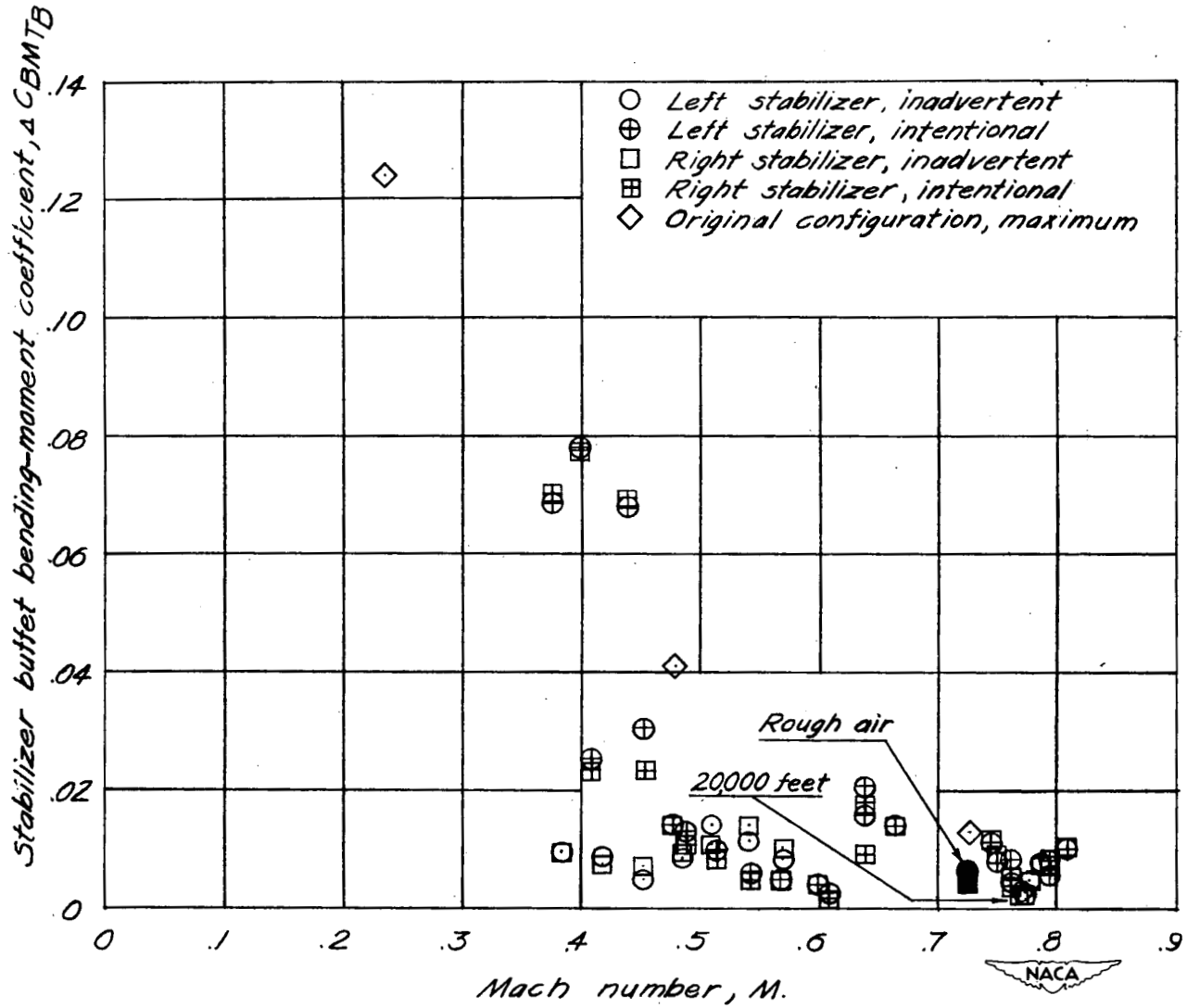

Figure 7.- Stabilizer buffeting bending-moment coefficients.

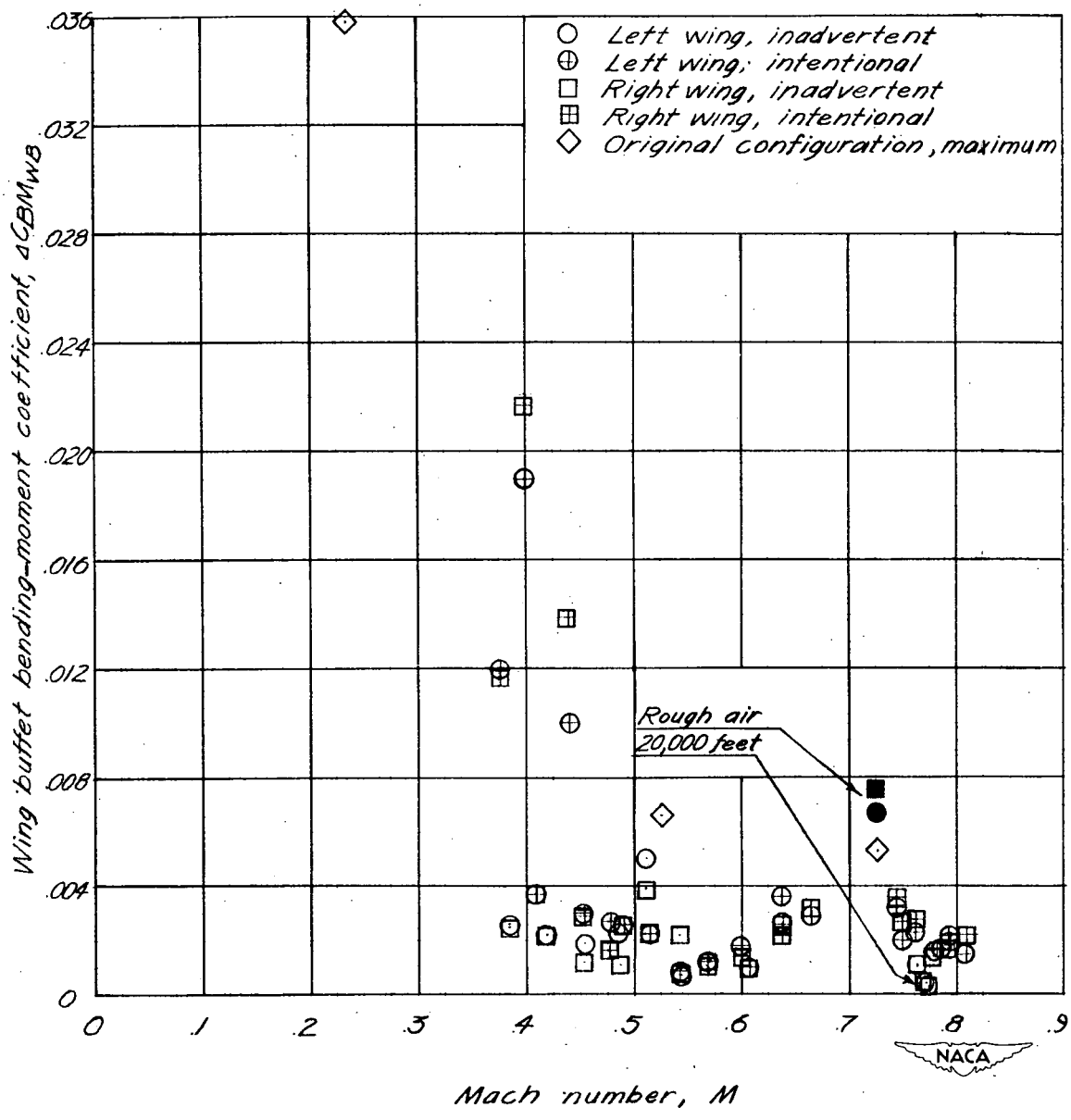

Figure 8.- Wing buffeting bending-moment coefficient.

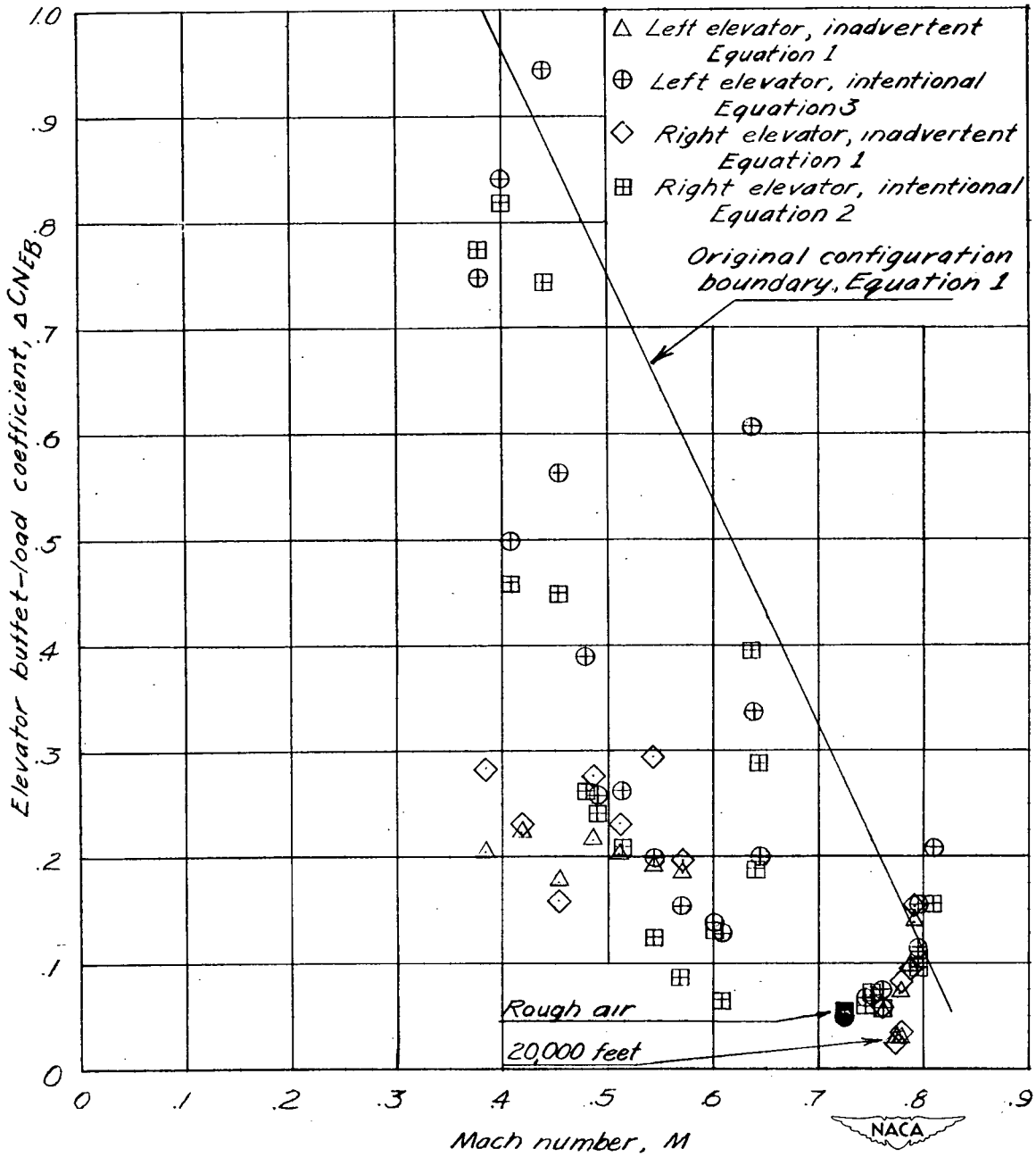

Figure 9.- Elevator buffeting-load coefficients.

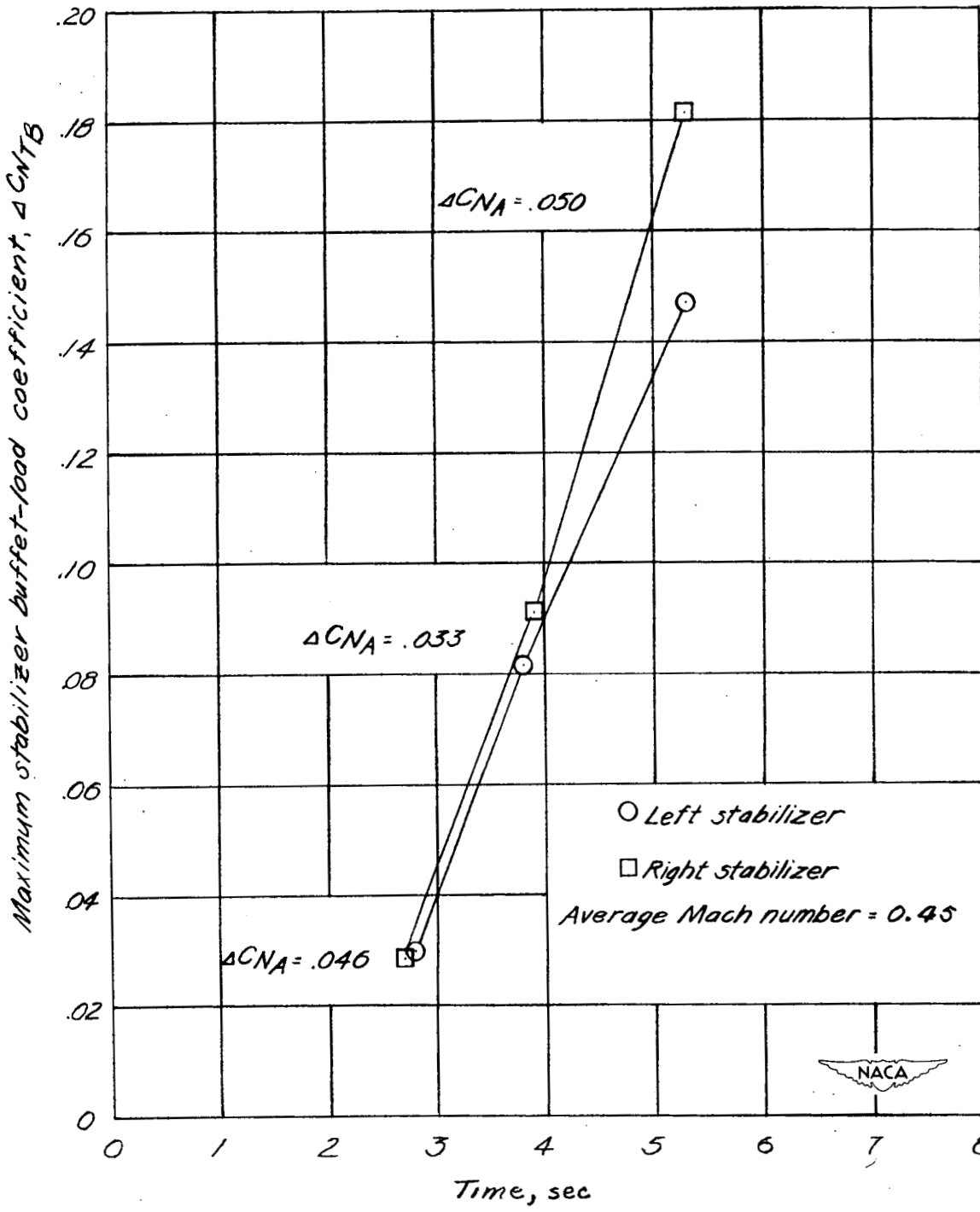

Figure 10.- Effect of time in buffeting on stabilizer buffet-load coefficient as illustrated by maximum buffet-load coefficients for each of three maneuvers.